

Hollow-core slabs with cast-in-place concrete toppings: A study of interfacial shear strength

Ryan M. Mones and Sergio F. Breña

Since the 1950s, prestressed concrete hollow-core slabs have been used in a variety of structural applications, including residential and commercial buildings, parking structures, and short-span bridges. The slabs contain voids that run continuously along their length, which helps reduce dead weight and material cost. **Figure 1** shows hollow-core slabs with two different top surface conditions.

Hollow-core slabs are economical, have good fire resistance and sound insulation properties, and are capable of spanning long distances with relatively shallow depths. Common depths of prestressed hollow-core slabs range from 6 to 10 in. (150 to 250 mm) for spans of approximately 30 ft (9 m). More recently, hollow-core slabs with depths as great as 16 in. (410 mm) have become available and are capable of spanning more than 50 ft (15 m).

In practice, a concrete topping layer is often cast in place onto the top surface of hollow-core slabs to create a continuous level finished surface. The topping layer is typically 2 in. (50 mm) deep. The topping may increase the flexural strength, shear strength, and bending stiffness of the slab if composite action is developed with the hollow-core units.

Composite action between the cast-in-place concrete topping and the hollow-core unit is developed primarily through bond at the interface. Steel reinforcement to promote composite action across concretes cast at differ-

- This paper reports tests on two types of hollow-core units (dry mix and wet mix) to determine the interfacial shear strength between them and their cast-in-place concrete toppings.
- Tests conducted using push-off specimens designed to generate shear stresses at the interface showed that interfacial shear strength correlates with surface roughness, sandblasting to remove laitance (from wet-mix specimens), and grouting.



Specimen with machine-finished surface



Longitudinally raked slab

Figure 1. Hollow-core slabs.

ent times is not practical for this application because of the automated fabrication process of hollow-core units. Interface shear strength may potentially be increased by roughening the precast concrete surface before placement of the topping. The American Concrete Institute's *Building Code Requirements for Structural Concrete (ACI 318-11) and Commentary (ACI 318R-11)*¹ currently limits the design horizontal shear strength of unreinforced, intentionally roughened composite interfaces to a maximum of 80 psi (0.55 MPa) but fails to define what constitutes an intentionally roughened surface. Section 5.3.5 of the *PCI Design Handbook: Precast and Prestressed Concrete*² states that experience and testing indicate that normal finishing methods used for precast concrete surfaces may be considered as intentionally roughened surfaces for design purposes.

The objective of this research was to investigate the influence of surface preparation techniques on interface shear strength between hollow-core slabs and cast-in-place concrete toppings. With a better estimate of interfacial shear strength, the flexural and shear strength benefits associated with composite action between hollow-core units and cast-in-place concrete toppings could be exploited. Only those techniques that were practically feasible were included in this study, though several are not commonly performed. Several past studies³⁻⁶ have focused on determining the interfacial shear strength of concrete cast at different times and having different surface roughnesses, with and without transverse reinforcement crossing the interface. Previous researchers have also tested hollow-core slabs with composite topping,⁷⁻⁹ but the primary focus of these studies has been to determine the flexural and shear strength of the composite units. Past researchers have not specifically focused on the interfacial shear strength between hollow-core units and cast-in-place concrete toppings, with the units fabricated using typical producer practices. The main goal of this research project was to provide experimental

data in this area.

Experimental program

Twenty-four specimens representing two different methods of hollow-core slab production were tested. The two producers that fabricated the hollow-core units use different fabrication machines and therefore employ different concrete mixtures in their processes. One producer uses an extruder with a dry-mix concrete, and the other uses a slip form machine with a wet-mix concrete. These two types were selected to broaden the applicability of the research results. The laboratory specimens were constructed using short segments of hollow-core units onto which a cast-in-place concrete block representing the topping concrete was placed. The hollow-core units were fabricated with different surface conditions to determine the influence of surface roughness on interface shear strength.

Specimen description

Testing was conducted on push-off specimens consisting of two blocks of concrete cast at different times. The bottom block, a 36 in. (910 mm) long hollow-core segment, was fabricated in a hollow-core producer facility and shipped to the laboratory. The top block was cast in the laboratory directly on the bottom block using a concrete strength that would typically be encountered in toppings. **Figure 2** shows specimen geometry and dimensions.

The push-off specimens were designed to ensure that applied loads only generated shear stresses along the surface between bottom and top blocks without creating any normal stresses. Therefore, the top block had to be cast into an L-shape and a structural steel assembly was embedded into the bottom block at the fabrication facility (**Fig. 3**).

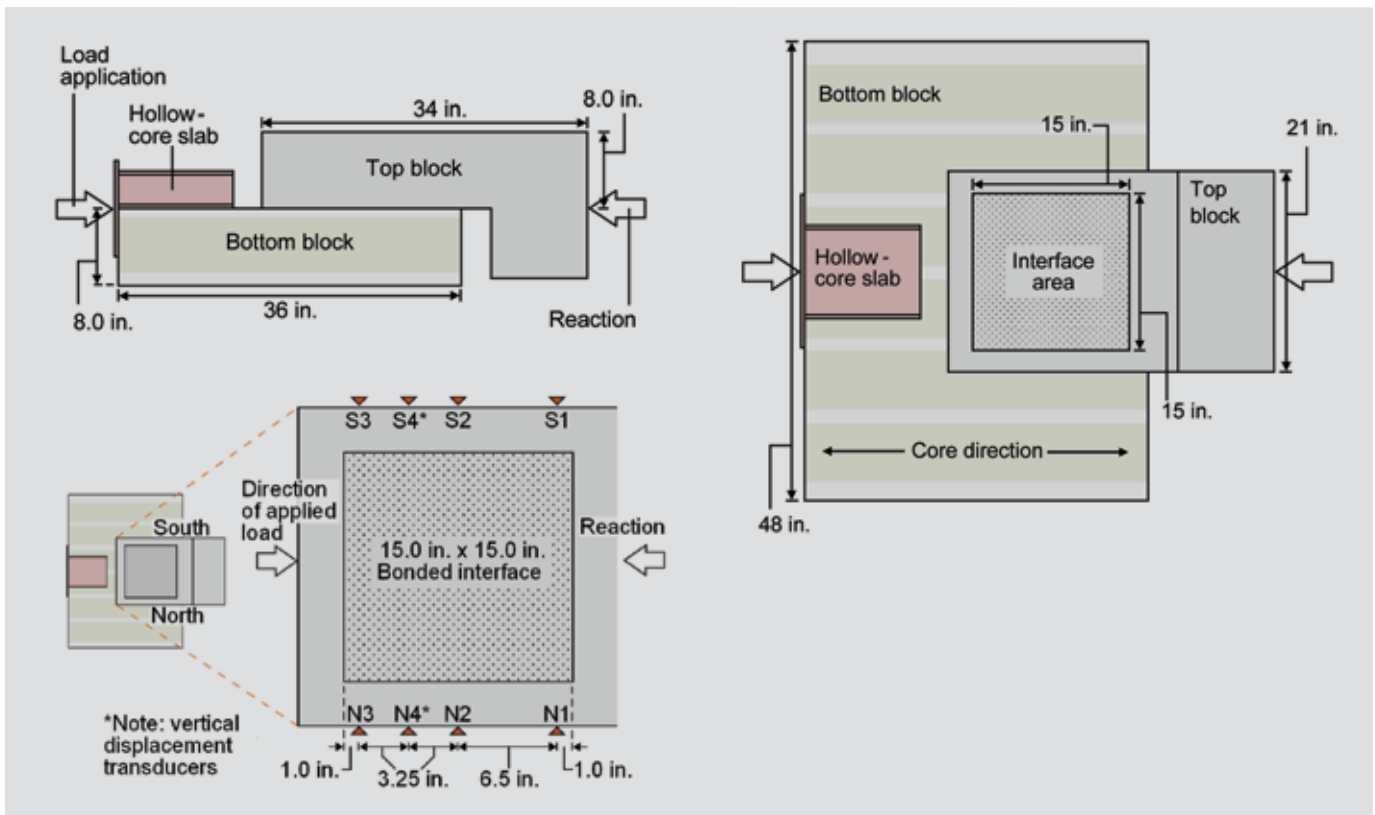


Figure 2. Dimensions of push-off specimens and instrumentation location. Note: 1 in. = 25.4 mm.

The test region of the specimens consisted of a 15 × 15 in. (380 × 380 mm) surface in the central region of the contact area between the top and bottom blocks. This test region is smaller than the total contact area between blocks (Fig. 2). The contact surface outside of the test region was intentionally debonded using plastic and smooth tape. The geometry of the top block was designed to ensure that the top block weight would not generate significant normal stresses on the test area.

Table 1 lists the finishing process used on the top surface of the bottom blocks. Top surface conditions included machine-finished surfaces, longitudinally raked surfaces, longitudinally or transversely broomed surfaces, and sandblasted surfaces, with grout added to some of those surfaces (**Fig. 4**). Duplicate bottom blocks were fabricated and tested for each surface condition. Surface roughening was performed at the hollow-core fabrication plant. Grout was applied onto the test region of



Structural steel assembly insert in dry-mix longitudinally raked specimen DRY-LRX-1



Side view of specimen before testing

Figure 3. Views of bottom and top blocks in specimens.

Table 1. Specimen labels, concrete material strengths, and surface roughness measurements

Specimen label	Surface condition	Top block compressive strength, psi	Top block splitting tensile strength, psi	Bottom block compressive strength, psi
DRY-MFX-1	Machine finished	4670	420	6920
DRY-MFX-2		3780	360	7170
DRY-SBX-1	Sandblasted	4510	410	7310
DRY-SBX-2		5000	440	7740
DRY-LRX-1	Longitudinally raked	4630	420	7600
DRY-LRX-2		5020	450	8010
DRY-TBX-1	Transversely broomed	4750	450	7450
DRY-TBX-2		5140	480	7880
DRY-MFG-1	Machine finished, grouted	4670	410	8150
DRY-MFG-2		5050	440	8430
DRY-LRG-1	Longitudinally raked, grouted	4820	450	8290
DRY-LRG-2		5110	440	8580
WET-MFX-1	Machine finished	5180	440	9700
WET-MFX-2		5180	450	9730
WET-SBX-1	Sandblasted	4960	430	9750
WET-SBX-2		4530	440	9760
WET-LBX-1	Longitudinally broomed	5190	450	9720
WET-LBX-2		4810	410	9780
WET-TBX-1	Transversely broomed	4930	410	9810
WET-TBX-2		4140	470	9830
WET-MFG-1	Machine finished, grouted	4310	420	9850
WET-MFG-2		5420	420	9880
WET-LBG-1	Longitudinally broomed, grouted	4510	380	9900
WET-LBG-2		4100	370	9920

Note: 1 psi = 6.985 kPa.

four specimens for each of the two fabrication processes (wet-mix and dry-mix). Only specimens with machine-finished and longitudinally roughened surfaces were selected for grout application. In grouted specimens, a commercial nonshrink sand-cement grout was applied in a layer approximately $1/16$ in. (1.6 mm) thick in the laboratory using a steel trowel and roughened using a stiff broom. The grout was allowed to dry 24 to 48 hours before casting the top block. Pressurized air was used to remove loose particles from the top surface of the bottom block before application of grout.

The top surface of machine-finished specimens remained as produced by the fabrication machine without further

finishing. Machine-finished specimens therefore capture roughness conditions that are typical of the two hollow-core production methods investigated and properties of the concrete mixture. The surface of the dry-mix longitudinally raked specimens was roughened using a rake attached to the hollow-core extruder that was dragged along the surface before concrete setting. All other roughened specimens were roughened by hand.

All dry-mix bottom blocks were cast on the same day using the same batch of concrete. Most wet-mix bottom blocks were also cast on a single day using a single batch except for wet-mix longitudinally broomed specimen WET-LBX-2, which was cast one week later.

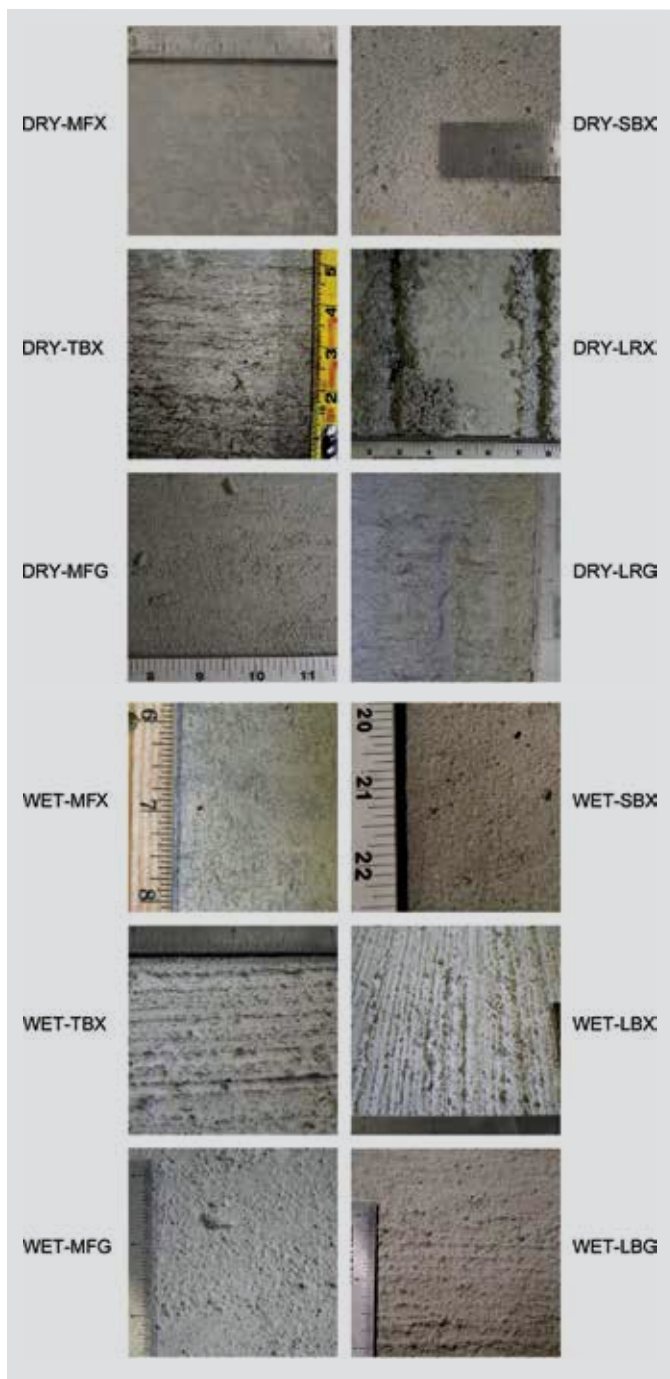


Figure 4. Bottom block surface condition of dry- and wet-mix specimens.

Materials

To avoid damaging the interface during handling in the laboratory, the top blocks were cast after the bottom blocks were positioned in the testing frame. The top blocks were fabricated using concrete with a design compressive strength of 4000 psi (27.6 MPa). The top block concrete mixture had a maximum aggregate size of $\frac{3}{8}$ in. (10 mm) that reflects characteristics of common topping concrete mixtures. The day before placing the top block concrete, the surface of the bottom block was saturated with water. Standing water was blotted dry prior to placing concrete.

Mechanical vibration was used to compact the top block concrete after placement. The top block was cured at room temperature (approximately 70°F [20°C]) with wet burlap and plastic for 48 hours after casting. The wet burlap remained on the blocks after formwork removal and was removed approximately 24 hours before testing. Push-off specimens were typically tested 6 days after casting the top block.

For each top block, three 4 × 8 in. (100 × 200 mm) cylinders were tested in compression in accordance with ASTM C39, *Standard Test Method for Compressive Strength of Cylindrical Concrete Specimens*,¹⁰ and two 6 × 12 in. (150 × 300 mm) cylinders were tested to determine splitting tensile strength in accordance with ASTM C496, *Standard Test Method for Splitting Tensile Strength of Cylindrical Concrete Specimens*.¹¹ These cylinders were subjected to the same curing conditions as their companion top block. Each hollow-core slab manufacturer provided a total of twelve 4 × 8 in. (100 × 200 mm) concrete cylinders that were fabricated using the same batch of concrete as the bottom blocks. Compressive strength testing of these cylinders was conducted at different times throughout the duration of the entire set of tests from each manufacturer to determine concrete strength at different times and allow estimation of the strength of each hollow-core slab at the time of testing. The cylinders were kept in the laboratory under the same environmental conditions as the bottom blocks. Table 1 lists the top block compressive strength, splitting tensile strength, and bottom block compressive strength, determined on the testing day of each specimen. Compressive strength of the grout was determined by testing 2 in. (50 mm) cubes in accordance with ASTM C109, *Standard Test Method for Compressive Strength of Hydraulic Cement Mortars*.¹²

Specimen instrumentation and testing procedure

Relative movement between the top and bottom blocks was measured using linear potentiometers, six positioned in the direction of loading and two positioned normal to the interface plane (Fig. 2). The six longitudinal transducers measured horizontal displacement between top and bottom blocks. They were fixed along the two sides (north and south) of the top block. The two vertical transducers were installed on either side of the top block to measure vertical movement of the top block relative to the bottom block in 19 of the 24 specimens (**Table 2**). A 110 kip (490 kN) load cell was used at the end of the actuator to measure applied force. Readings of all instruments were recorded every 2 seconds. Specimens were loaded monotonically until failure. The rate of loading was not controlled during the tests, but tests took from 6.5 to 11 minutes to conduct. Figure 3 shows a side view of one of the specimens fixed to the testing frame.

Table 2. Summary of experimental results

Specimen label	Surface condition	Maximum force, kip	Interface shear strength, psi	Horizontal slip at failure, in.	Vertical displacement at failure, in.	Mean macrotex-ture depth of test area (bottom block), in.	Mean macrotex-ture depth of grout surface, in.
DRY-MFX-1	Machine finished	46.5	207	0.0006	not recorded	0.0099	n/a
DRY-MFX-2		34.2	152	0.0001	not recorded	0.0094	n/a
DRY-SBX-1	Sandblasted	36.4	162	0.0010	not recorded	0.0113	n/a
DRY-SBX-2		48.4	215	0.0017	0.0003	0.0122	n/a
DRY-LRX-1	Longitudinally raked	50.2	223	0.0021	not recorded	0.0221	n/a
DRY-LRX-2		46.1	205	0.0013	0.0012	0.0233	n/a
DRY-TBX-1	Transversely broomed	64.7	288	0.0018	not recorded	0.0294	n/a
DRY-TBX-2		71.8	319	0.0034	0.0018	0.0326	n/a
DRY-MFG-1	Machine finished, grouted	62.0	276	0.0016	0.0011	0.0086	0.0208
DRY-MFG-2		84.8	377	0.0029	0.0017	0.0087	0.0208
DRY-LRG-1	Longitudinally raked, grouted	62.2	276	0.0029	0.0013	0.0215	0.0270
DRY-LRG-2		59.8	266	0.0026	0.0012	0.0193	0.0270
WET-MFX-1	Machine finished	44.6	198	0.0014	0.0002	0.0146	n/a
WET-MFX-2		28.7	128	0.0009	0.0002	0.0149	n/a
WET-SBX-1	Sandblasted	60.2	268	0.0019	0.0006	0.0173	n/a
WET-SBX-2		50.6	225	0.0024	0.0007	0.0173	n/a
WET-LBX-1	Longitudinally broomed	49.9	222	0.0019	0.0006	0.0423	n/a
WET-LBX-2		32.4	144	0.0011	0.0002	0.0366	n/a
WET-TBX-1	Transversely broomed	57.9	257	0.0025	0.0010	0.0474	n/a
WET-TBX-2		55.7	248	0.0022	0.0005	0.0400	n/a
WET-MFG-1	Machine finished, grouted	35.4	157	0.0010	0.0001	0.0130	0.0208
WET-MFG-2		37.2	165	0.0015	0.0004	0.0130	0.0208
WET-LBG-1	Longitudinally broomed, grouted	55.6	247	0.0021	0.0009	0.0380	0.0210
WET-LBG-2		49.1	218	0.0021	0.0006	0.0359	0.0210

Note: n/a = not applicable. 1 in. = 25.4 mm; 1 kip = 4.448 kN; 1 psi = 6.985 kPa.

Surface roughness quantification

Surface roughness plays an important role in interface shear strength. In the past, however, mostly qualitative statements have been used to describe concrete surface roughness conditions. It was therefore considered important to develop a method for potential use in the field that would provide a quantifiable measure of surface roughness conditions.

A surface roughness quantification method was established by adapting a standard test method used for roughness measurement in pavements. The method, referred to as the sand patch test, was adapted from ASTM E965, *Standard Test for Measuring Pavement Macro-texture Depth Using a Volumetric Technique*.¹³ The test involves spreading a known volume of well-graded sand onto the roughened surface in a circular pattern using a rubber spreading disc. Spreading continues until the sand patch size no longer increases. The diameter of the sand patch is measured at four

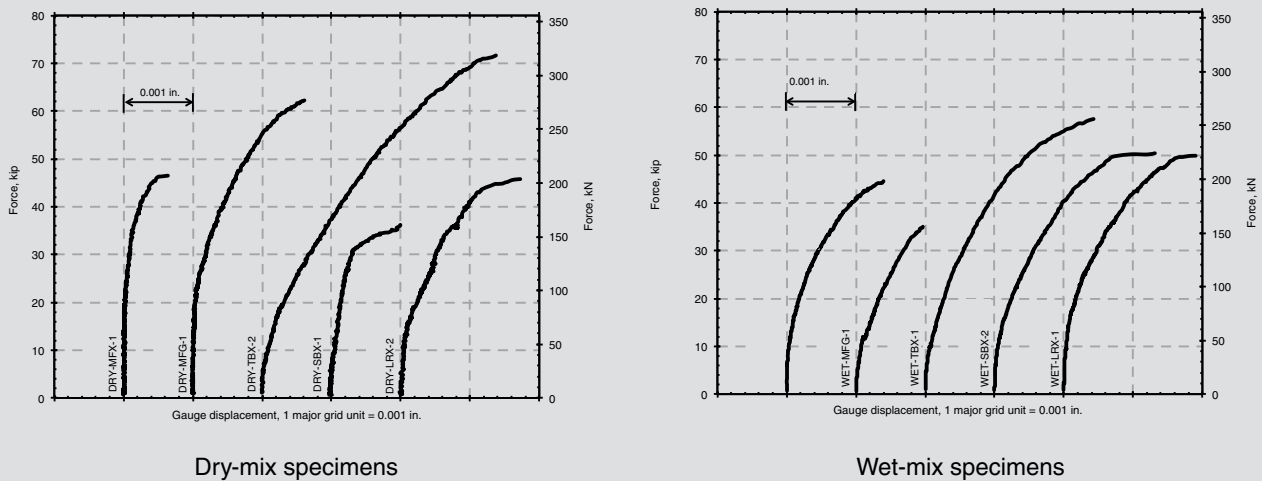


Figure 5. Comparison of force-displacement plots of selected specimens. Note: 1 in. = 25.4 mm.

different locations. The average diameter of the sand patch is related to the macrotexture depth of the surface, which represents one-half the average depth between the bottom of surface voids and the top of the surface aggregate particles (Eq. [1]). To account for experimental variability, each test was repeated four times for each specimen surface in the laboratory, and a mean macrotexture depth was defined by averaging the results from the four tests.

$$MTD = \frac{4V}{\pi D^2} \quad (1)$$

where

MTD = macrotexture depth

V = volume of sand used in the measurement

D = average diameter of the sand patch

ASTM E965 specifies using sand passing a no. 50 (0.297 mm) sieve and retained on a no. 100 (0.149 mm) sieve for pavement surfaces. Because concrete surfaces have smaller voids and a tighter pore structure than asphalt pavement, sand passing a no. 100 sieve and retained on a no. 200 (0.074 mm) sieve was used instead. A sand volume of 1 in.³ (16,000 mm³) was more suitable for use on the precast concrete surfaces used in this research than the 2 in.³ (131,000 mm³) specified by ASTM E965. A rubber disc with a diameter of 3.0 in. (75 mm) and weight of 0.36 lb (160 g) was used to spread the sand.

One limitation of the sand patch test is that it is unreliable when the concrete surface is highly irregular, such as in rake-roughened surfaces, because the rubber disk cannot be maintained in a horizontal position. In these specimens, the mean macrotexture depth was approximately determined by measuring the rake grooves using a vernier caliper. The depth probe of the vernier caliper was used to measure the

depth between the bottom of the rake grooves and the top of the concrete ridges along the grooves created during the raking process. Groove widths were measured using the inside jaws of the vernier caliper. Rake groove depths and ridge heights were measured at 9 different locations throughout the test area, resulting in 18 different measurements for each raked specimen.

Results of laboratory testing

Failure of all specimens was sudden and brittle, without visual indications of impending failure. All push-off specimens failed cleanly along the interface plane. No cracks were observed on either the top or bottom blocks before failure of any specimen.

Table 2 gives a summary of test results from the push-off specimens, including maximum applied shear force, average interfacial shear stress at maximum force, average horizontal slip at failure measured by gauges N1 and S1, and average vertical displacement of top block at failure measured by gauges N4 and S4. The average interface shear stress was calculated by dividing the maximum force into the test area of the specimens (15 × 15 in. [380 × 380 mm]). All specimens had an interface shear strength that far exceeded 80 psi (0.55 MPa), the limit specified in section 17.5.3.1 of ACI 318-11 for intentionally roughened surfaces without transverse reinforcement crossing the interface. The specimens with the lowest interface shear strength in each group, dry-mix machine-finished specimen DRY-MFX-2 and wet-mix machine-finished specimen WET-MFX-2, exceeded the 80 psi limit by factors of 1.9 and 1.6, respectively. The average interface shear strength of all specimens was 227 psi (1.57 MPa). Table 2 shows the variability in interface shear strength.

Table 2 also lists the mean macrotexture depth of the bottom block surface of each specimen. For grouted speci-

mens, the mean macrotexture depth was also determined on the surface of the grout after hardening (Table 2). Grout fragments adhered to the top block after failure in the grouted specimens, indicating good bond between blocks. This observation dispelled concerns about the presence of grout weakening the bond at the interface. **Figure 5** shows typical sets of force-displacement plots. Horizontal and vertical displacements, when present, were obtained by averaging the readings from instruments attached to the north and south faces at each instrumented location. The largest slips were generally measured in the first row of transducers except for dry-mix longitudinally raked specimen DRY-LRX-2, in which the second row of instruments recorded the highest displacements. The vertical displacements, though small, were of similar magnitude to the smallest horizontal displacements registered in each push-off specimen, consistent with the findings of Seible and Latham.¹⁴ Vertical displacements occurred primarily at high loads, so they were likely caused by movement of the top block as it displaced over surface irregularities of the bottom block at horizontal displacements approaching failure.

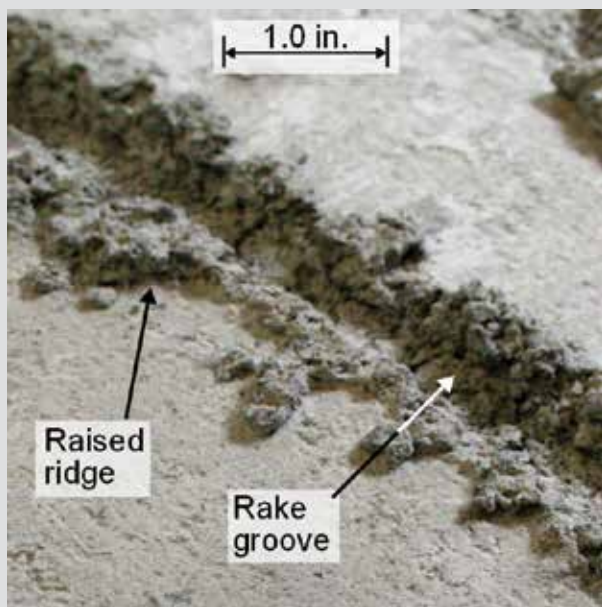
Of the four machine-finished specimens, only dry-mix machine-finished specimen DRY-MFX-1 exhibited areas of exposed aggregate on the surface of the top block. This specimen had the highest strength of all machine-finished specimens, but not significantly higher than wet-mix machine-finished specimen WET-MFX-1.

The dry-mix longitudinally raked specimens had deep grooves that were approximately 0.25 in. (64 mm) deep and spaced at 5 in. (130 mm) on center. The concrete that

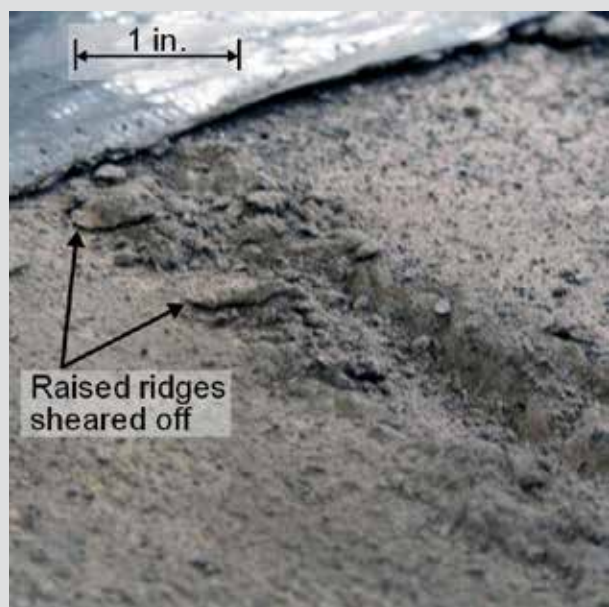
was displaced during raking collected along the edge of each groove, forming raised ridges of hardened concrete along the grooves. These ridges sheared from the top surface of the bottom blocks after failure (**Fig. 6**). The concrete that filled the grooves during casting of the top block did not shear from the top block during loading, perhaps because the grooves were parallel to the direction of load application.

Broom-roughened surfaces had the highest mean macrotexture depth of all surface conditions. The average mean macrotexture depth of the dry-mix and wet-mix broom-roughened specimens was 0.0310 in. (0.787 mm) and 0.0416 in. (1.06 mm), respectively. Variations in brooming techniques and concrete properties resulted in significantly different average mean macrotexture depth between the dry-mix and wet-mix specimens. Transversely broom-roughened specimens had the highest interfacial shear strength and horizontal slip capacity among all nongrooved dry- and wet-mix specimens. Ridges that were formed in these specimens by brooming in a direction perpendicular to the applied shear force promoted interlocking between the top and bottom blocks.

Dry-mix sandblasted specimens and wet-mix sandblasted specimens were sandblasted at the plant after the hollow-core slab segments had hardened. As reflected by the mean macrotexture depth values, sandblasting only increased the surface roughness of the bottom blocks compared with machine-finished companion specimens by a small amount. The average mean macrotexture depth of the dry-mix and wet-mix sandblasted specimens was 22% and 17% higher than the corresponding machine-finished surfaces, respective-



Before testing



After testing

Figure 6. Rake groove on the bottom block surface of dry-mix longitudinally raked specimen DRY-LRX-1. Note: 1 in. = 25.4 mm.

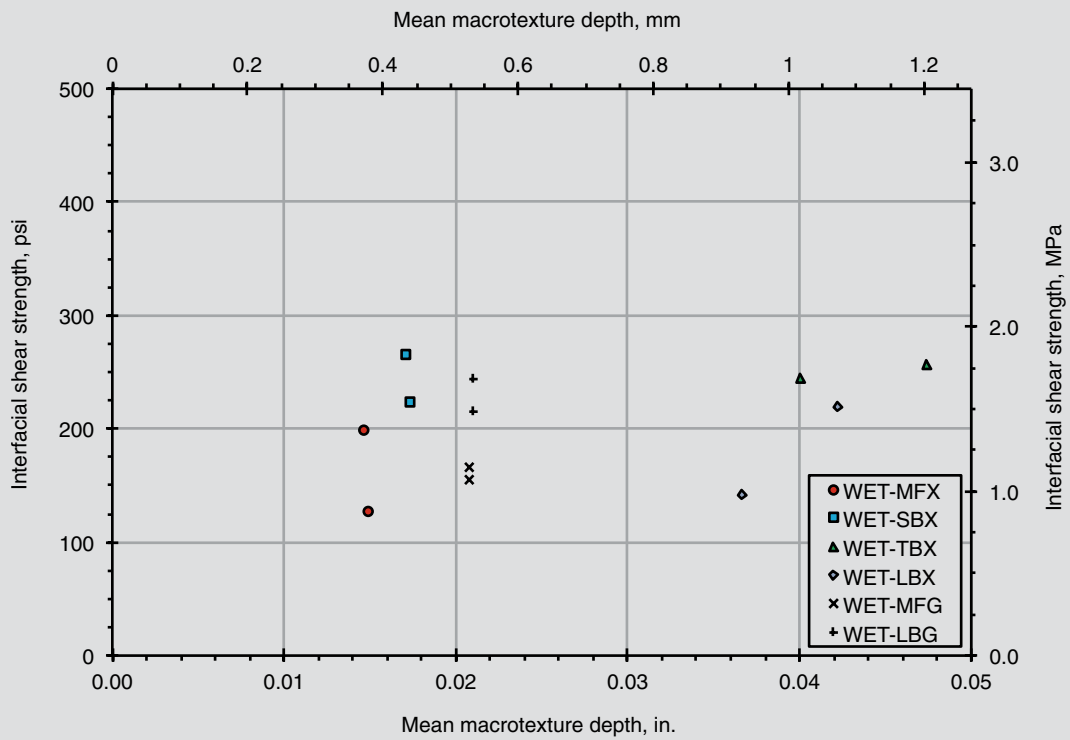
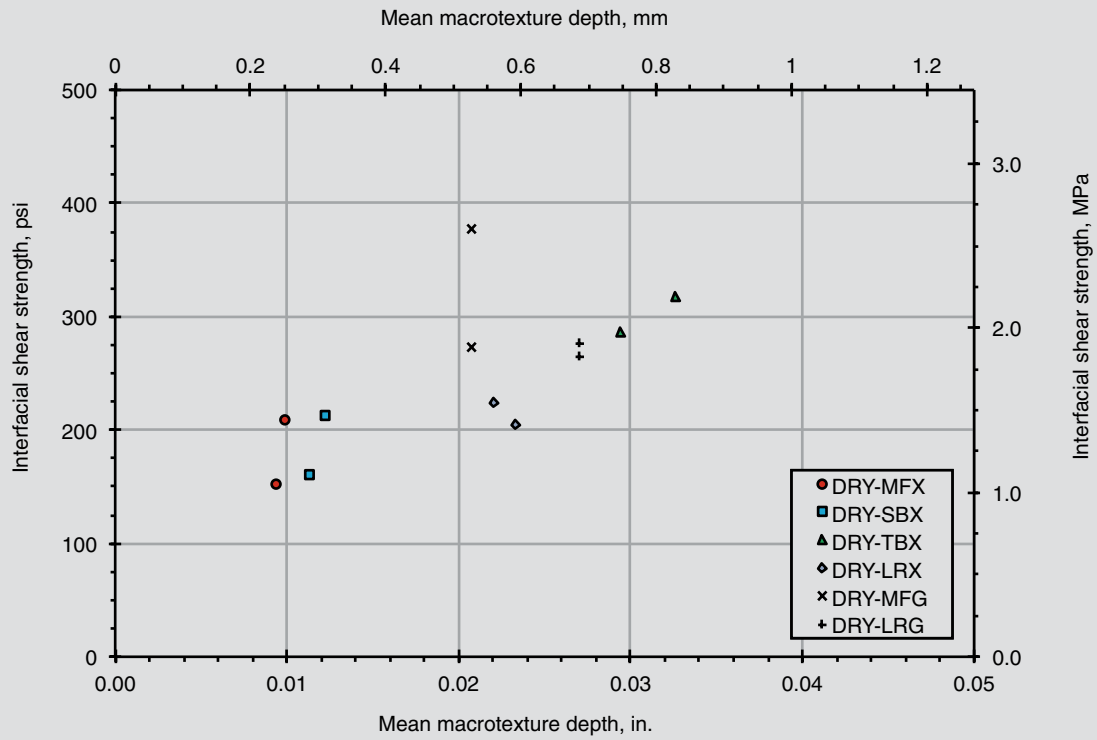


Figure 7. Relationship between mean macrottexture depth and interfacial shear strength.

ly. The sandblasting process removed a thin layer of concrete from the surface of the bottom block. This layer often contains laitance and other debris that may detract from the bond quality of the interface. Compared with dry-mix machine-finished specimens, dry-mix sandblasted specimens had higher slip capacity and nearly equal interfacial shear strength. Wet-mix sandblasted specimens had, on average, 51% higher interfacial shear strength and 86% higher horizontal slip capacity compared with corresponding wet-mix machine-finished specimens. Higher laitance content was observed in wet-mix sandblasted specimens than in dry-mix sandblasted specimens attributing to the higher benefit of sandblasting in wet-mix specimens as would be expected because of differences in the concrete mixtures used during fabrication.

The grouted dry-mix machine-finished specimens had higher interfacial shear strength and horizontal slip capacity than ungrouted companion specimens. Grouted specimens had higher mean macrotexture depth values compared with the dry-mix machine-finished and dry-mix longitudinally raked specimens (140% and 32%, respectively, on average). Furthermore, dry-mix machine-finished grouted and dry-mix longitudinally raked grouted specimens had average interfacial shear strengths approximately 82% and 27% higher, respectively, than corresponding specimens that were not grouted. Inspection of the failure surfaces of the dry-mix grouted specimens revealed regions where grout remained bonded to the bottom block, regions where the grout remained bonded to the top block, and regions where a thin layer of the top block concrete (along with the grout) remained bonded to the bottom block. This gave evidence of adequate bond between the grout and the two blocks.

The wet-mix machine-finished grouted specimens did not exhibit a marked increase in interfacial shear strength or horizontal slip capacity compared with companion specimens without grout, despite an average increase in mean macrotexture depth of 60% on the grouted surface. The mean macrotexture depth of wet-mix longitudinally broomed grouted specimens was 43% lower than the surface before grouting but had 27% higher average interfacial shear strength than the companion specimens without grout. There was high variability of interface shear strength in individual specimens. In the wet-mix machine-finished grouted specimens, the entire layer of grout remained bonded to the top block except for a small 3 × 4 in. (75 × 100 mm) area that remained bonded to the bottom block. This may have been a result of the surface concrete characteristics of the bottom block that resulted from the wet-mix process, as will be discussed in more detail in the next section.

Influence of roughness on interfacial shear strength

Figure 7 shows the relationship between interfacial shear strength and mean macrotexture depth. For grouted specimens, the mean macrotexture depth values plotted were

measured on the grouted surface. Data in these figures are average values of replicate specimens. A strong linear correlation can be observed between mean macrotexture depth and interface shear strength of dry-mix specimens. The correlation coefficient between interface shear strength and mean macrotexture depth of dry-mix specimens is 0.69. In contrast, a weak linear correlation between interface shear strength and mean macrotexture depth was obtained for the wet-mix specimens, with a correlation coefficient of 0.28.

The surface of the wet-mix bottom blocks generally contained more laitance than the surface of dry-mix specimens. Laitance typically accumulated within valleys of the roughness undulations of wet-mix specimens, particularly when the surface was broomed. Removal of concrete laitance from the surface, as specified by section 17.5.3.1 of ACI 318-11, would have required an abrasive technique. Instead, to avoid disturbing the surface conditions of the bottom blocks significantly, reasonable attempts to remove laitance were made by brushing and blowing with compressed air. Presence of laitance may have caused the higher variability observed in strength results of replicate wet-mix specimens and may have also contributed to the lower average interface strengths at a given mean macrotexture depth compared with dry-mix specimens. Significantly higher interfacial shear strength was obtained in wet-mix sandblasted specimens compared with wet-mix machine-finished specimens, indicating that sandblasting effectively removed surface laitance.

Further evidence of the detrimental effect of laitance is found from the test results of the wet-mix longitudinally broomed specimen WET-LBX-2. This specimen was cast on a different date from others in this group, and the bottom block surface of this specimen had higher laitance content. This specimen had a lower mean macrotexture depth, significantly lower interfacial shear strength, and lower horizontal slip at failure than any other broom-roughened specimen. If test results of the wet-mix longitudinally broomed specimen WET-LBX-2 are omitted from the wet-mix data, the correlation coefficient between interface shear strength and mean macrotexture depth increases to 0.45, still a low value. These results highlight the importance of proper laitance removal for adequate bond of a topping. Interfacial shear strength also increased with horizontal slip at failure (**Fig. 8**). The least-squares linear relationship for these data was found with a correlation coefficient between shear strength and slip of 0.80.

Parameters affecting strength of composite hollow-core slabs

Nominal strength of composite hollow-core slabs may be governed by shear, loss of composite action (horizontal shear failure), or flexural capacity depending on material and geometric properties. The governing mode of failure

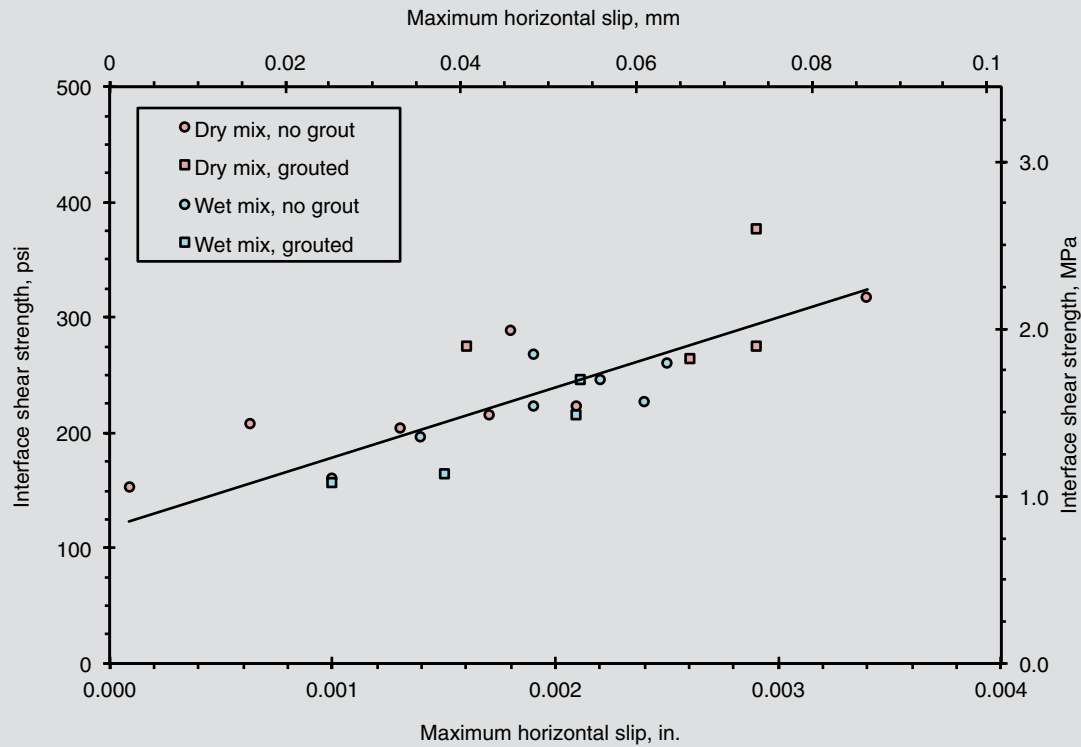


Figure 8. Relationship between interface shear strength and horizontal slip at failure.

depends on parameters such as span, depth, flexural-to-shear strength ratio, and material strength. Nominal strengths are affected by a strength reduction factor ϕ equal to 0.75 for shear and 0.90 for flexural failures.

A study to identify the parameters that affect strength of different hollow-core sections was conducted to identify the conditions for which horizontal shear strength is critical.

Shear strength of hollow-core sections

Hollow-core sections do not usually contain transverse reinforcement, so the nominal shear strength is calculated relying only on the concrete contribution as the smaller of web-shear cracking V_{cw} and flexural-shear cracking V_{ci} in accordance with section 11.3 of ACI 318-11.

These failure modes govern at different sections along the hollow-core unit depending on proximity to the support and presence of concentrated forces. At a given section, the minimum value computed by Eq. (11-10), (11-11), and (11-12) in ACI 318-11 determines the vertical shear strength of hollow-core slabs.

$$V_{ci} = 0.6\sqrt{f'_c}b_w d_p + V_d + \frac{V_i M_{cre}}{M_{max}} \quad (11-10)$$

where

$$f'_c = 28\text{-day concrete compressive strength}$$

b_w = summation of web widths measured at midheight

d_p = depth to centroid of prestressing steel

V_d = shear due to dead loads

V_i = shear acting simultaneously with M_{max} at section i

M_{cre} = cracking moment at section i , accounting for effects f_{pe} and f_d

f_{pe} = effective prestressing stress

f_d = stress induced by permanent (dead) loads

M_{max} = maximum factored moment at section i

$$M_{cre} = \left(\frac{I}{y_t} \right) \left(6\sqrt{f'_c} + f_{pe} - f_d \right) \quad (11-11)$$

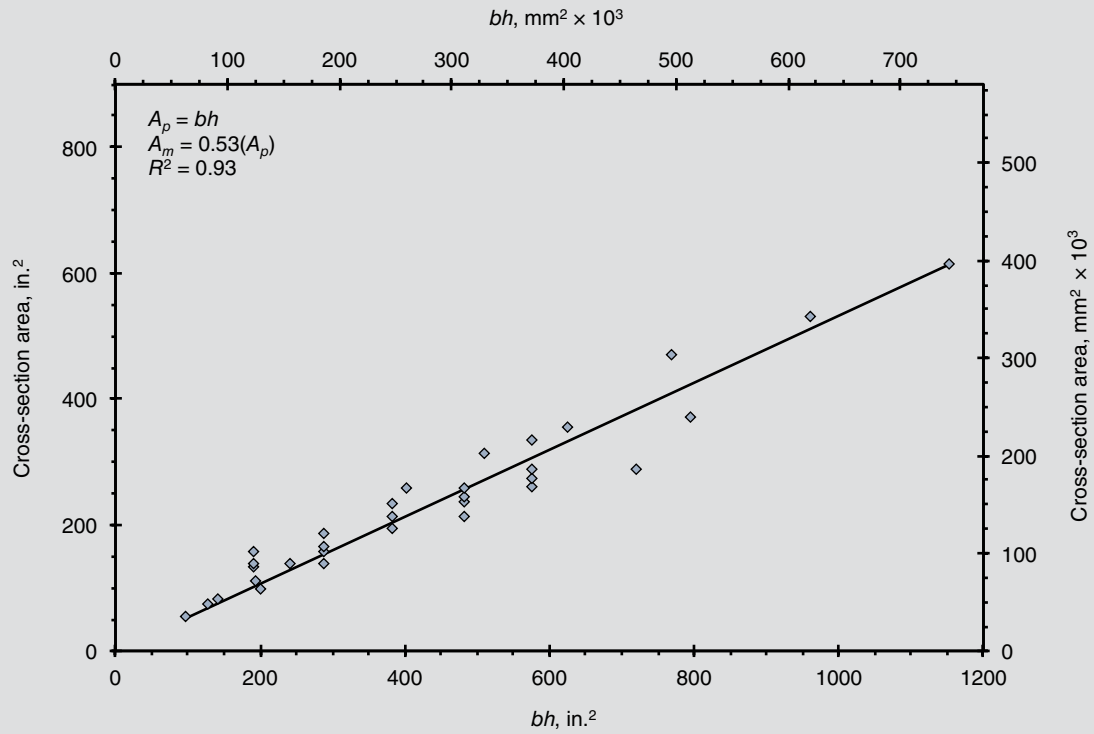
where

I = moment of inertia

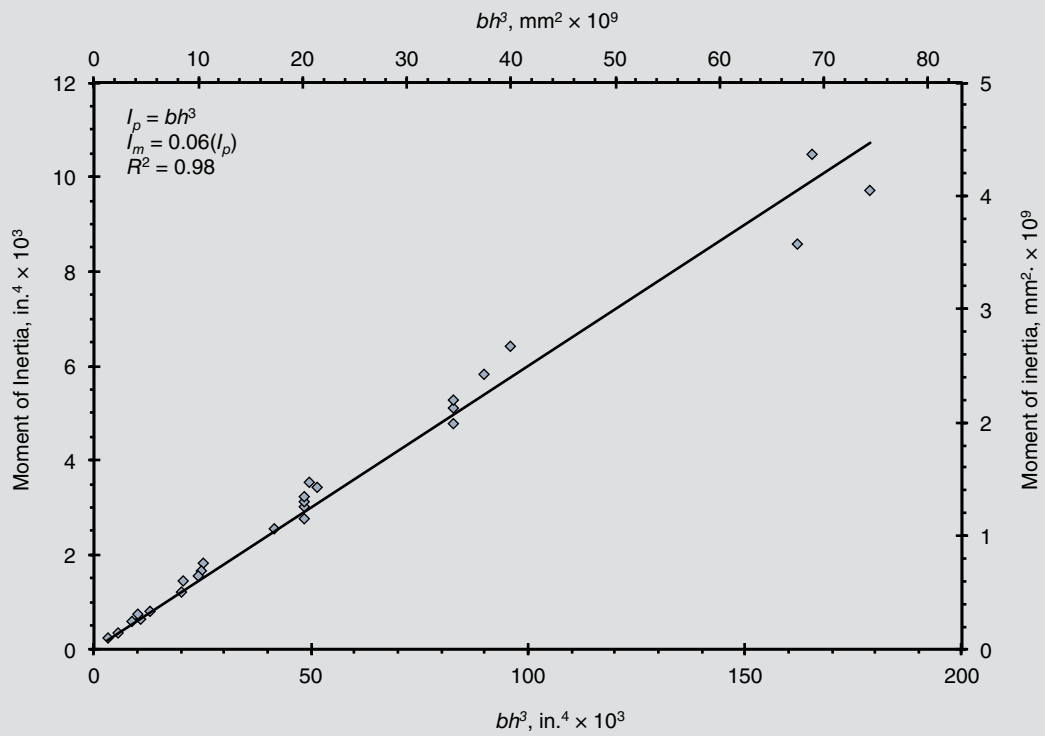
y_t = distance from centroid of section to tensile face

$$V_{cw} = \left(3.5\sqrt{f'_c} + 0.3f_{pc} \right) b_w d_p + V_p \quad (11-12)$$

f_{pc} = stress at centroid of the cross section induced by prestressing and noncomposite moments



Area



Moment of inertia

Figure 9. Cross-sectional properties used for parametric hollow-core units. Note: A_m = model-predicted cross-section area; A_p = parameter related to area as defined in the figure; b = width of hollow-core slab; h = depth of hollow-core slab; I_m = model-predicted moment of inertia; I_p = parameter related to moment of inertia as defined in the figure; R = correlation coefficient to least-squares fit.

V_p = contribution of prestressing reinforcement to shear strength (zero for straight strands)

The shear strength of sections near the support where shear forces are high is usually governed by V_{cw} (Eq. 11-12).

Horizontal shear strength of composite hollow-core sections

The nominal horizontal shear strength of unreinforced, intentionally roughened composite interfaces is calculated using ACI 318-11, section 17.5.3.1, in accordance with Eq. (2):

$$V_{nh} = 80b_v d \quad (2)$$

where

V_{nh} = nominal horizontal shear strength of interface

b_v = composite interface contact width

d = depth of composite section

The factored shear force at any section may not exceed the design strength ϕV_{nh} . Alternatively, the factored horizontal shear force transferred along the composite interface can be computed from the change in compressive force in the topping layer between two sections (ACI 318-11 section 17.5.4). *PCI Design Handbook* section 5.3.5 suggests calculating the change in compression force between the sections of zero moment and maximum moment. If the *PCI Design Handbook* procedure is used, design horizontal shear strength is determined using Eq. (1) by substituting the composite contact surface for $b_v d$.

Using the method in the *PCI Design Handbook* is equivalent to calculating the average horizontal shear stress along the composite interface throughout the shear span. The use of an average horizontal shear stress for design relies on the redistribution capacity of the interface as shear stresses reach the interfacial shear strength. The capacity to redistribute stresses is perhaps higher in interfaces crossed by reinforcement but may be limited in unreinforced surfaces because of their low slip capacity.

Flexural strength of hollow-core sections

Flexural strength of hollow-core sections is calculated using common assumptions used for flexural design and a strand stress f_{ps} calculated using Eq. (18-1) in ACI 318-11:

$$f_{ps} = f_{pu} \left\{ 1 - \frac{\gamma_p}{\beta_1} \left[\rho_p \frac{f_{pu}}{f'_c} + \frac{d}{d_p} (\omega - \omega') \right] \right\} \quad (18-1)$$

where

f_{pu} = nominal strength of prestressing strand

γ_p = factor for type of prestressing steel = 0.28 for f_{py}/f_{pu} not less than 0.90

f_{py} = yield stress of prestressing steel

β_1 = factor relating depth of equivalent rectangular stress block to neutral axis depth

ρ_p = prestressing steel reinforcement ratio = A_{ps}/bd

ω = mechanical reinforcement ratio of mild reinforcement = $\rho f_y / f'_c$

ρ = reinforcement ratio of mild reinforcement

ω' = mechanical reinforcement ratio of mild reinforcement in compression = $\rho' f_y / f'_c$

ρ' = reinforcement ratio of mild reinforcement in compression

The hollow-core sections used in this research did not contain any mild reinforcement (tensile or compressive), so the second term within the square brackets in Eq. (18-1) was omitted.

Compressive stresses were replaced by an equivalent rectangular stress block in accordance with ACI 318-11 section 10.2.7.

Parametric study

A parametric study was conducted to estimate the maximum superimposed live load that different generic hollow-core slab cross sections can support without reaching flexural, vertical shear, or horizontal shear failure for a range of simply supported spans. The cross-sectional properties of the generic hollow-core slabs used in this study were established from models created from actual hollow-core slabs tabulated in the *PCI Manual for the Design of Hollow-core Slabs*.¹⁵ These models were created to capture general behavior of the large variety of hollow-core shapes available in the market to make the results of this study widely applicable independent of the hollow-core producer.

The two main cross-sectional parameters chosen to create the generic hollow-core section models were area and moment of inertia. Hollow-core areas from individual producers were plotted against the area of a rectangle enclosing the plank bh , where b is width and h is depth (**Fig. 9**). Similarly, moments of inertia of hollow-core slabs from different producers were plotted as a function of bh^3 . The

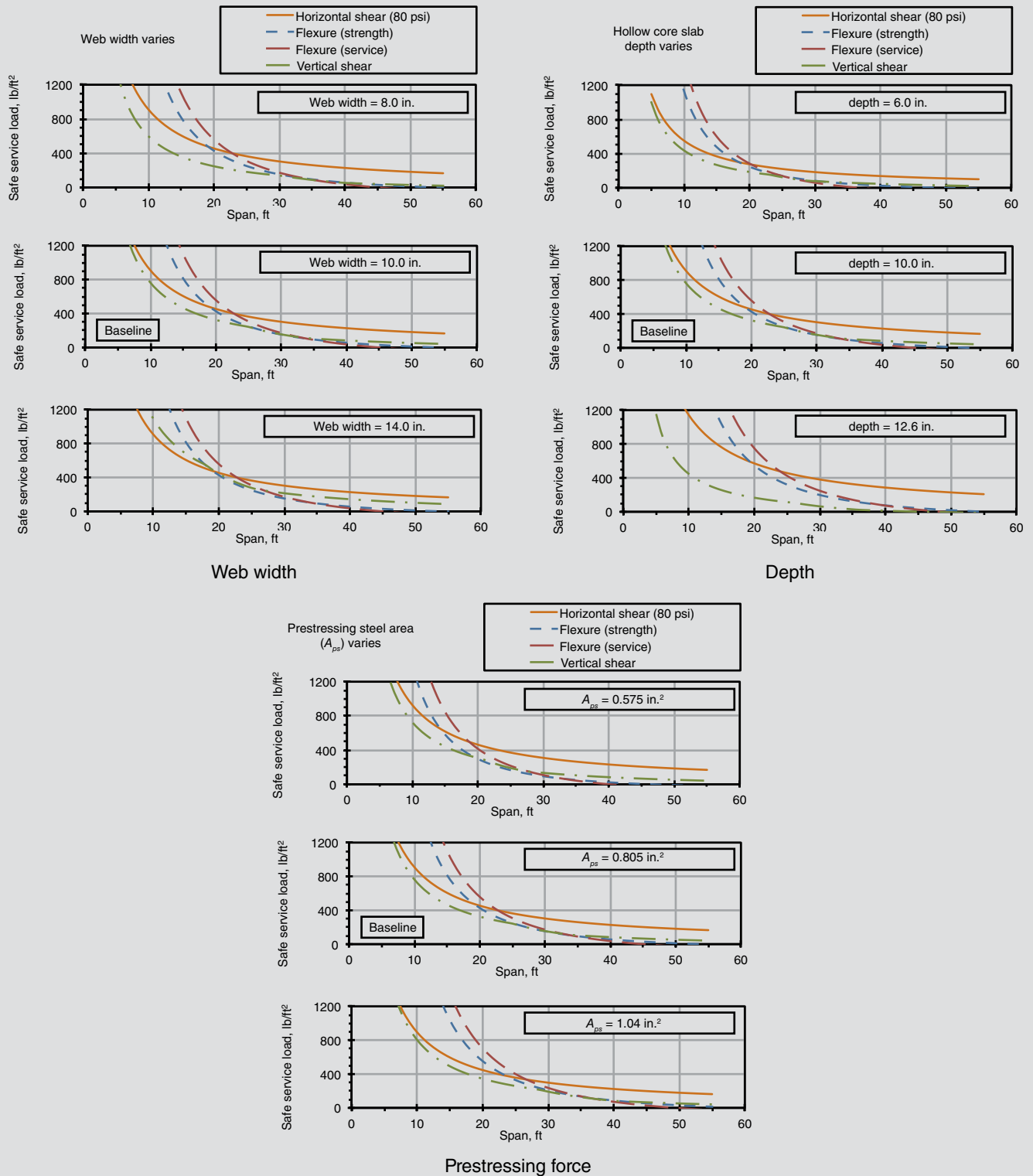


Figure 10. Effects of selected parameters on strength of hollow-core slabs. Note: Except where variance is noted, properties were constant: hollow-core slab width = 4 ft; hollow-core slab depth = 10 in.; hollow-core slab web width = 10 in.; hollow-core slab concrete compressive strength = 5000 psi; prestressing steel strength = 270 ksi; prestressing steel area = 0.0805 in.²; topping slab thickness = 2.0 in.; topping slab concrete compressive strength = 4000 psi. 1 in. = 25.4 mm; 1 ft = 0.305 m; 1 lb = 4.448 N; 1 psi = 6.985 kPa.

relationship between area or moment of inertia of hollow-core slabs and the enclosing rectangle was established through linear regression. For any given width b and depth h of a hollow-core slab, the area A_m and moment of inertia

I_m of the modeled cross section were determined using the results from this regression analysis, thereby eliminating the need to use manufacturer-specific data.

Table 3. Baseline composite hollow-core slab properties

Baseline hollow-core slab	
Depth	10 in.
Width	4.0 ft
Web width*	10 in.
Compressive strength f'_c	5000 psi
Depth to bottom strands	8.75 in.
Area	256 in. ²
Moment of inertia	2880 in. ⁴
Weight	67 lb/ft ²
Prestressing steel (in hollow-core slab)	
Number of strands	7
Strand diameter	7/16 in.
Nominal strength f_{pu}	270 ksi
Initial pull	75%
Total loss	18%
Strand type	7-wire, low relaxation
Topping slab	
Thickness	2 in.
Compressive strength f'_c	4000 psi
Effective width	43 in.
Weight	25 lb/ft ²
Composite section	
Depth	12 in.
Width	4 ft
Depth to bottom strands	10.75 in.
Effective area	340 in. ²
Moment of inertia	5222 in. ⁴
Weight	92 lb/ft ²

*Web width is the sum of the widths of all webs of the hollow-core slab.
 Note: 1 in. = 25.4 mm; 1 ft = 0.305 m; 1 lb = 4.448 N;
 1 psi = 6.895 kPa; 1 ksi = 6.895 MPa.

A baseline composite hollow-core slab cross section was defined to allow comparisons with other sections modified by changing selected parameters. The baseline hollow-core section properties were chosen to represent a typical hollow-core slab widely manufactured by many producers. Additional cross sections, defined in this paper as parametric hollow-core sections, were generated by changing a single design property of the baseline section (material or

cross-sectional property) while keeping all other properties constant. **Table 3** lists the baseline hollow-core slab material and cross-sectional properties.

The minimum distributed live load required to reach flexural, shear, and horizontal shear strength was calculated for each parametric hollow-core section for span lengths ranging from 5.0 to 55.0 ft. (1.5 to 16.8 m). Strengths were determined using equations from ACI 318-11 and the *PCI Design Handbook* when applicable, as discussed previously. Top- and bottom-fiber stresses were also determined at service-load levels (full dead and live load) and compared with allowable values in the *PCI Design Handbook* to determine the allowable distributed live load. **Figure 10** shows selected results of the parametric study. These figures depict the relationship between maximum distributed service live load that can be applied for a given span length without violating service or strength design requirements.

Results from the parametric study show that short- to medium-span hollow-core slabs, typically ranging from 5.0 to 25 ft (1.5 to 7.6 m), are controlled by shear. At longer spans, hollow-core slabs were governed by service-level flexural stresses. Horizontal shear strength was found to be critical only in slabs with high vertical shear strength, such as those with higher web widths (Fig. 10), for spans less than approximately 20 ft (6.1 m). Hollow-core slabs with narrower web widths are governed by vertical shear for spans up to 30 ft (9.1 m) or by flexure for longer spans. An interfacial shear stress of 80 psi (0.55 MPa) was used to determine the horizontal shear strength of slabs in accordance with Eq. (2). If a higher interfacial shear stress were used consistent with tests conducted in this research, shear strength would not govern for the range of variables studied in this research. The results of this study are limited to simply supported slabs with distributed live load.

Conclusion

This research investigated the effect of surface roughening on the strength of the composite interface between precast concrete hollow-core slabs and cast-in-place concrete topping layers. This was accomplished through a testing program involving 24 push-off specimens with varying surface conditions of the base block. Dry-mix and wet-mix hollow-core slabs were tested. There was no reinforcement crossing the interface between the bottom and top blocks. The following conclusions are drawn from the results of this study:

- For dry-mix hollow-core slabs, a strong positive linear correlation was observed between surface roughness and interfacial shear strength and horizontal slip capacity. Based on observations, the interfacial shear strength of wet-mix hollow-core slabs was related to both surface roughness and the presence of laitance.

- Sandblasting removed the laitance layer from the wet-mix hollow-core slabs and improved interfacial shear strength by providing a higher quality cohesive bond and, to a lesser extent, increasing the surface roughness.
- Roughened interfaces developed higher strength and horizontal slip capacity than machine-finished interfaces. Roughening was most effective when grooves were perpendicular to the applied shear force.
- The interfacial shear stress limit of 80 psi (0.55 MPa) specified in ACI 318-11 for intentionally roughened surfaces is conservative for all surface conditions tested, including machine-finished specimens. Test results show that higher shear strengths of unreinforced composite interfaces can be obtained by roughening the hardened concrete surface.
- Grout did not impair the interfacial shear strength of dry-mix and wet-mix hollow-core slab surfaces. In fact, grouted dry-mix specimens had significantly higher interfacial shear strength and horizontal slip capacity than companion specimens that were not grouted. Grouted wet-mix specimens had moderate increases in interfacial shear strength compared with companion specimens that were not grouted.
- Analysis of simply supported hollow-core slabs under distributed loading shows that the capacity of short hollow-core slabs is typically governed by vertical shear strength. Horizontal shear strength only governs in short-span slabs with thick webs.

To further validate the results reported in this paper, the authors believe that large-scale tests of full-length hollow-core slabs with cast-in-place concrete toppings would be invaluable.

Acknowledgments

The research reported in this paper was made possible through a PCI Daniel P. Jenny Student Fellowship. The authors would like to thank the partner producer members, Oldcastle Precast in South Bethlehem, N.Y., and J.P. Carrara and Sons of Middlebury, Vt., who provided the hollow-core slab specimens. We are grateful to Barker Steel in Deerfield, Mass., which donated reinforcement for construction of top blocks in the laboratory. Deep gratitude is extended to members of the research advisory panel, in particular to Paul Kourajian, who served as chair of the panel and to David Wan, who provided significant feedback throughout the planning phase of the project. The constructive feedback from other members of the research advisory panel is gratefully recognized.

References

1. ACI (American Concrete Institute) Committee 318. 2011. *Building Code Requirements for Structural Concrete (ACI 318-11) and Commentary (ACI 318R-11)*. Farmington Hills, MI: ACI.
2. PCI Industry Handbook Committee. 2010. *PCI Design Handbook: Precast and Prestressed Concrete*. MNL 120. 7th ed. Chicago, IL: PCI.
3. Hanson, N. W. 1960. "Precast-Prestressed Concrete Bridges 2. Horizontal Shear Connections." *Journal of the PCA Research and Development Laboratories* 2 (2): 38–57.
4. Djazmati, B., and J. A. Pincheira. 2004. "Shear Stiffness and Strength of Horizontal Construction Joints." *ACI Structural Journal* 101 (4): 484–493.
5. Julio, E. N. B. S., F. A. B. Branco, and V. D. Silva. 2004. "Concrete-to-Concrete Bond Strength. Influence of the Roughness of the Substrate Surface." *Construction and Building Materials* 18 (9): 675–681.
6. Kovach, J. D., and C. Naito. 2008. "Horizontal Shear Capacity of Composite Concrete Beams without Interface Ties." ATLSS report 08-05, ATLSS Center, Lehigh University, Bethlehem, Pa.
7. Scott, N. L. 1973. "Performance of Precast Prestressed Hollow-core Slab with Composite Concrete Topping." *PCI Journal* 18 (2): 64–77.
8. Ueda, T., and B. Stitmannathum. 1991. "Shear Strength of Precast Prestressed Hollow Slabs with Concrete Topping." *ACI Structural Journal* 88 (4): 402–410.
9. Girhammar, U. A., and M. Pajari. 2008. "Tests and Analysis on Shear Strength of Composite Slabs of Hollow Core Units and Concrete Topping." *Construction and Building Materials* 22 (8): 1708–1722.
10. ASTM Subcommittee C09.61. 2012. *Standard Test Method for Compressive Strength of Cylindrical Concrete Specimens*. ASTM C39. West Conshohocken, PA: ASTM International.
11. ASTM Subcommittee C09.61. 2011. *Standard Test Method for Splitting Tensile Strength of Cylindrical Concrete Specimens*. ASTM C496. West Conshohocken, PA: ASTM International.
12. ASTM Subcommittee C01.27. 2011. *Standard Test Method for Compressive Strength of Hydraulic Cement Mortars (Using 2-in. or [50 mm] Cube Specimens)*. ASTM C109. West Conshohocken, PA: ASTM International.

mens). ASTM C109. West Conshohocken, PA: ASTM International.

13. ASTM Subcommittee E17.23. 2006. *Standard Test Method for Measuring Pavement Macro-texture Depth Using a Volumetric Technique*. ASTM E965. West Conshohocken, PA: ASTM International.
14. Seible, F., and C. T. Latham. 1990. "Horizontal Load Transfer in Structural Concrete Bridge Deck Overlays." *Journal of Structural Engineering* 116 (10): 2691–2710.
15. Buettner, D. R., and R. J. Becker. 1998. *Manual for the Design of Hollow Core Slabs*. 2nd ed. Chicago, IL: PCI.

Notation

A_m = model-predicted cross-section area

A_p = parameter related to area

b = width of hollow-core slab

b_v = composite interface contact width

b_w = sum of all web widths measured at midheight

d = depth of composite section

D = average diameter of the sand patch in the macrotexture depth test

d_p = depth to centroid of prestressing steel

f'_c = 28-day concrete compressive strength

f_d = stress induced by permanent (dead) loads

f_{pc} = stress at centroid of the cross section induced by prestressing and noncomposite moments

f_{pe} = effective prestressing stress

f_{ps} = strand stress

f_{pu} = nominal strength of prestressing steel

f_{py} = yield stress of prestressing steel

h = depth of hollow-core slab

I = moment of inertia

I_m = model-predicted moment of inertia

I_p = parameter related to moment of inertia

M_{cre} = cracking moment at section i , accounting for effects of prestressing f_{pe} and presence of permanent loads f_d

M_{max} = maximum factored moment at section i

MTD = macrotexture depth

R = correlation coefficient to least-squares fit

V = volume of sand used in macrotexture depth test

V_{ci} = flexural-shear cracking

V_{cw} = web-shear cracking

V_d = shear due to dead loads

V_i = shear acting simultaneously with M_{max} at section i

V_{nh} = nominal horizontal shear strength of interface

V_p = contribution of prestressing reinforcement to shear strength (zero for straight strands) y_i = distance from centroid of section to tensile face

β_1 = factor relating depth of equivalent rectangular stress block to neutral axis depth

γ_p = factor for type of prestressing steel = 0.28 for f_{py}/f_{pu} not less than 0.90

ρ = reinforcement ratio of mild reinforcement

ρ' = reinforcement ratio of mild reinforcement in compression

ρ_p = prestressing steel reinforcement ratio = A_{ps}/bd

ϕ = strength reduction factor

ω = mechanical reinforcement ratio of mild reinforcement = $\rho f_y / f'_c$

ω' = mechanical reinforcement ratio of mild reinforcement in compression = $\rho' f_y / f'_c$

About the authors



Ryan M. Mones, EIT, MS, is a staff engineer with Simpson, Gumpertz, and Heger in Boston, Mass. He was a research assistant at the University of Massachusetts–Amherst. His research interests include behavior of

prestressed concrete members and interface shear strength of concretes cast at different ages.



Sergio F. Breña, PhD, FACI, is an associate professor at the University of Massachusetts–Amherst. He is secretary of ACI committees 318C and 369, and a member of ACI 374 and the ACI Publications Committee. His research interests

include design and behavior of structural concrete, use of fiber-reinforced materials to strengthen structures, and short- and long-term monitoring of bridges.

Abstract

Precast concrete hollow-core slabs are often constructed with a cast-in-place concrete topping on site. Common construction practice includes applying cementitious grout between hollow-core units as a bonding agent. The cast-in-place concrete topping may con-

tribute to the strength and stiffness of the hollow-core slabs if composite action is developed. The strength of the interface between the hollow-core units and the cast-in-place concrete topping largely depends on the surface condition of the slabs because it is not feasible to provide transverse reinforcement in these elements. The research presented in this paper primarily includes testing of two types of hollow-core units (dry mix and wet mix) to determine the interfacial shear strength between the units and the cast-in-place concrete toppings. Tests were conducted using push-off specimens designed to generate shear stresses at the interface. A parametric study is also conducted to identify the governing failure mode of topped hollow-core slabs as a function of span length.

Keywords

Hollow-core, push-off testing, roughening, shear strength, topping.

Review policy

This paper was reviewed in accordance with the Precast/Prestressed Concrete Institute's peer-review process.

Reader comments

Please address any reader comments to journal@pci.org or Precast/Prestressed Concrete Institute, c/o PCI Journal, 200 W. Adams St., Suite 2100, Chicago, IL 60606. 